International Journal of Material Forming (2025) 18:52
https://doi.org/10.1007/s12289-025-01913-8

ORIGINAL RESEARCH

# The plastic flow analysis of cold strained DC04 ferritic steel using BBC family yield functions under associated flow rule and non-associated flow rule concepts

**Naoel Brinis[1] · Oualid Chahaoui[1] · Abdenour Saoudi[1] · Salim Boulahrouz[1] · Nedjoua Matougui[2]**

Received: 11 July 2024 / Accepted: 11 May 2025


**Abstract**
This study compares the mechanical properties of numerically predicted anisotropic parameters (using the BBC family of models) and experimentally measured results for DC04 steel sheets. The evolution of mechanical properties—such as flow stresses and Lankford coefficient—was analysed during initial plastic anisotropy and mechanical strain hardening in material forming. The results show that the evolution of mechanical properties under isotropic work hardening was predicted with respect to the selected strain levels during tensile testing of the steel. A proposed regression model effectively described the yield stress and *r-value* behaviour. The Lankford parameter was determined as an instantaneous value based on polynomial fitting of the transverse versus longitudinal true plastic strain curve. Using 08 and 16 independent orthotropic parameters, the BBC criteria family (2003_8p, 2005_8p, 2008_8p, and 2008_16p) was formulated and tested under a non-associated plasticity framework across different material orientations relative to the sheet's rolling direction. Vickers hardness was determined by hardness testing and measuring the two diagonal indentations. The aspect ratio, defined as the ratio of diagonal lengths in the longitudinal direction to those in the thickness direction, was linked to the Lankford coefficient. A strong correlation was observed between experimental hardness measurements and the material's anisotropic properties.

**Keywords** DC04 Steel · Anisotropic metal · Non-associated flow rule · BBC criterion family · Evolution yield hardening · Hardness Anisotropy relation

## Introduction

The grades of sheet steel used in the automotive industry have been continually evolving in last decades. Today, to meet the requirements of manufacturers, metallurgists are designing lighter steel vehicle structures that are more adapted to environmental constraints and have excellent strength/weight ratio. For various application reasons, rolled sheets of ferritic steel are largely intended for the automotive industry. This process is used in a number of applications requiring a good compromise between mechanical properties such as strength, rigidity and ductility. In order to pilot forming processes regarding these materials, the formability intervals need to be adequately determined. In general, the environmental temperature conditions governing the forming process and the geometry of the manufacturing tool have a strong influence on the structure and behaviour of the finished product, which, consequently, induce the plastic anisotropy characteristics of subsequent transformations for the desired dimensions and shape [1–3]. The heterogeneity of the various phenomenological mechanical loadings is a result of the complexity of microstructural changes [4, 5]. In this context, many studies focused on developing mathematical models that can precisely capture the mechanical behaviour of the material deformation process. Initially, the classical analytic expression for isotropic materials was based on the formulation of Von Mises, 1928 [6]. Subsequently, Hill48 [7] modified the von Mises expression and proposed a quadratic analysis for anisotropic materials with mutual orthonormal planes of symmetry. The procedure of identifying the material parameters is simple and the required

✉ Abdenour Saoudi
saoudi_abdenour@univ-khenchela.dz

[1] Laboratory of Engineering and Sciences of Advanced Materials (ISMA), Abbes Laghrour University Khenchela, 40004 Khenchela, Algeria

[2] L3M- École Nationale Supérieure Des Technologies Industrielles, Annaba, Algeria

Published online: 26 May 2025

experimental data can be measured using standard uniaxial tensile tests. The pioneered non-quadratic plastic flow functions for isotropic and anisotropic metallic structures were introduced by Hosford (1972, 1996) [8, 9].To describe the yield flow of a various metals and based on the transformation of linear functions, the anisotropic mechanical behaviour of metal sheets was modelled using the criterion of Karafillis and Boyce, 1993 [10]. After a decade, Hosford's formulation was further extended and improved by Barlat and Lian (1989) [11]. Later, based on the algebraic application of a linear transformation of the stress tensor involving numerous anisotropy parameters, a series of plasticity criteria was proposed by Barlat [12–15] and Banabic [16, 17].

Over the past few decades, various anisotropic yield criteria have been developed to describe the plastic behaviour of textured sheets. These criteria balance the simplicity and the flexibility of incorporating multiple material parameters. Notable examples include the model of Banabic et al. [18] (BBC2008 model), which was formulated as a finite series expansion, in addition to Barlat 2005 model (Yld2004-18p) [19] and Qi Hu et al. Poly6 criterion [20]. In the context of multi-scale modeling, crystallographic texture data have been integrated into phenomenological yield functions, as demonstrated by Barlat et al. (2011) with the Yld2011-27p criterion [21]. Further advancements include a 3D yield function based on a sixth-order polynomial formulation (Yoshida et al., 2013) [22], which offers enhanced flexibility in capturing the anisotropic behaviour of steel sheets. Additionally, Yoon et al. proposed the Poly4 yield criterion [23], combining anisotropic hardening with an analytical description under the associated flow rule. An analytical criterion for modeling anisotropy and yield differential effects in pressure-insensitive metals was developed by Cazacu [24]. For pressure-sensitive metals, Yoon et al. [25] introduced an asymmetric yield function formulated in terms of stress invariants. Further advancements include a normalised stress invariant-based yield criterion proposed by Hu et al. [26]. Additionally, Lou et al. [27] developed a yield function expressed through the three stress invariants, effectively capturing pressure sensitivity, Lode dependence, and the strength-differential effect on material strength.

It is important to note that in recent years, the previous different anisotropic plastic flow functions have been proposed under associated flow rule (AFR) with different levels of precision and unique objectives [28]**.** Nevertheless, it is not easy to simultaneously determine completely anisotropic properties using a single yield criterion, as stipulated by AFR, including yield stress and plastic strain orientations. Building on Hill's 1948 quadratic yield function, and aiming to describe both yielding and plastic flow behaviour, Stoughton [29–31] introduced a simple and elegant approach known as the non-associated flow rule (non-AFR). This approach utilizes two distinct functions: one for the flow criterion and another for the anisotropic plastic potential equation. The non-associated flow rule (non-AFR) is another method that can successfully model anisotropic plastic behaviour. In this regard, it excludes the plastic yielding limitation and governs flow loadings with same criterion using two distinct functions: one for the flow criterion and another for the anisotropic plastic potential equation. Based on the non-AFR hypothesis, several phenomenological yield functions have been developed to model the anisotropic behaviour of materials [32–35].

Accurately predicting the mechanical behaviour of materials necessitates phenomenological validation against experimental data across the sheet plane. The directional dependence of plastic deformation is characterized by plastic flow, which establishes the constitutive relationship between stress and strain increment [36]. Rolled sheets exhibit orthotropic anisotropy, characterized by three mutually orthogonal planes of symmetry. This anisotropic behaviour is fundamentally related to the Lankford effect [37]. Material anisotropy is quantified through the Lankford coefficient (*r-value*), representing the width-to-thickness plastic strain ratio during longitudinal tensile testing. This parameter reveals significant differences in mechanical behaviour depending on orientation. Notably, the compressive *r-value* increases with strain while the tensile counterpart shows gradual reduction. As plastic deformation progresses under proportional loading conditions, the *r-value* demonstrates evolving tension–compression asymmetry, highlighting the stress-state dependence of plastic flow behaviour [38].

For assessing local mechanical properties, the indentation method has become one of the most widely used techniques for estimating flow stress and tensile strength, owing to its quasi-non-destructive nature. Material hardness characterizes a material's resistance to localized plastic deformation under indentation loading. Within the strain-hardening regime of metallic materials, numerous empirical correlations between Vickers hardness measurements and flow stress have been established in different studies [39–43].

This study investigates the anisotropic mechanical behaviour of cold-rolled DC04 ferritic steel sheets through the analysis of stress and strain tensors under both associated flow rule (AFR) and non-associated flow rule (non-AFR) frameworks. Multiple formulations of the non-quadratic BBC yield criterion family (2003_8p, 2005_8p, 2008_8p, and 2008_16p) were employed to assess their suitability for modelling the material's mechanical response. Initial characterisation under plane stress conditions was conducted using all BBC criteria within an associated plasticity framework, with the Bauschinger effect neglected to facilitate experimental validation. Subsequent non-AFR analysis examined variations in anisotropic parameters through the implementation of three BBC yield criteria (excluding BBC 2008_16p). The investigation further examined mechanical

strain hardening and initial plastic anisotropy, characterizing the evolution of both flow stresses and the Lankford coefficient during forming. Instantaneous flow stresses were calculated at specified equivalent strain levels using the Hockett-Sherby hardening model, while the Lankford coefficient was determined as an instantaneous value through polynomial fitting of strain data.

To assess plastic deformation resistance, Vickers hardness (*Hv*) testing was conducted, revealing a correlation between the Vickers indentation aspect ratio and the Lankford coefficient, offering a novel approach to characterizing mechanical anisotropy through hardness measurements. The established empirical relationship between Hv and ultimate tensile strength (UTS) was confirmed, with the *Hv*/UTS ratio typically approximating three, and the measured values ranging between 2.3 and 3.7.

## Experimental procedure

### Material and specimen

In this study, a cold-rolled DC04-grade steel sheet (ASTM A620; NE10130-2006) was used after being supplied by the Algerian Tractors Company (ATC), which is specialised in agricultural machinery. This material was selected for its widespread application in automotive body panel manufacturing. The chemical composition of the DC04 steel sheet was determined by optical emission spectrometry (SPECTROMAXx arc/spark OESKleve, Germany) and is presented in Table 1.

The specimens were extracted from the thin sheet using a high-power fiber laser cutting machine; the cutting direction was oriented at 15° between the rolling direction (RD) and transverse direction (TD).

### Measurement of σ(θ)-yield stress and r-value by tensile test

To assess the predictive capability of the yield functions, the material parameters were determined through uniaxial tensile testing. The experimental data included:

(1) $\sigma(\theta)$—yield stress (where $\sigma_{xx} = \sigma$ is the sole non-zero stress tensor component in the specimen coordinate system $X_1$, $X_2$, $X_3$; see Fig. 1-a).
(2) $r(\theta)$—anisotropy coefficient ($r(\theta) = \varepsilon_{yy}(\theta)/\varepsilon_{zz}(\theta)$, representing the plastic strain ratio [37].

These parameters were evaluated at seven material orientations relative to the rolling direction (RD): (0° = RD), 15°, 30°, (45° = diagonal direction, DD), 60°, 75°, and (90° = transverse direction, TD). The equibiaxial yield stress was approximated as: ($\sigma_b = (\sigma_0 + \sigma_{90})/2$), while the equibiaxial anisotropy coefficient $r_b = \varepsilon_{yy}/\varepsilon_{xx}$ was computed using the Yld96 yield criterion.

Tensile specimens were precision-machined from the sheet material and tested on a Hoytom 100 kN universal testing machine at a constant strain rate of $0.2 \times 10^{-3}$ $s^{-1}$ under ambient conditions. For statistical reliability, three rectangular specimens were tested for each orientation (gauge dimensions: 50 mm length × 12.5 mm width × 1.5 mm thickness; see Fig. 1-b).

The data plotted in Fig. 2 represent the engineering stress–strain curves obtained for seven different orientations, with the rotation angle between the uniaxial tensile test

**Table 1** Chemical composition of DC04 steel sheet (in wt%)

| Elements | C | Si | Mn | P | S | Mo | Al | Cu | Ti | Fe |
|---|---|---|---|---|---|---|---|---|---|---|
| Wt. % | 0.06 | 0.05 | 0.19 | 0.012 | 0.011 | 0.01 | 0.039 | 0.051 | 0.004 | Bal |

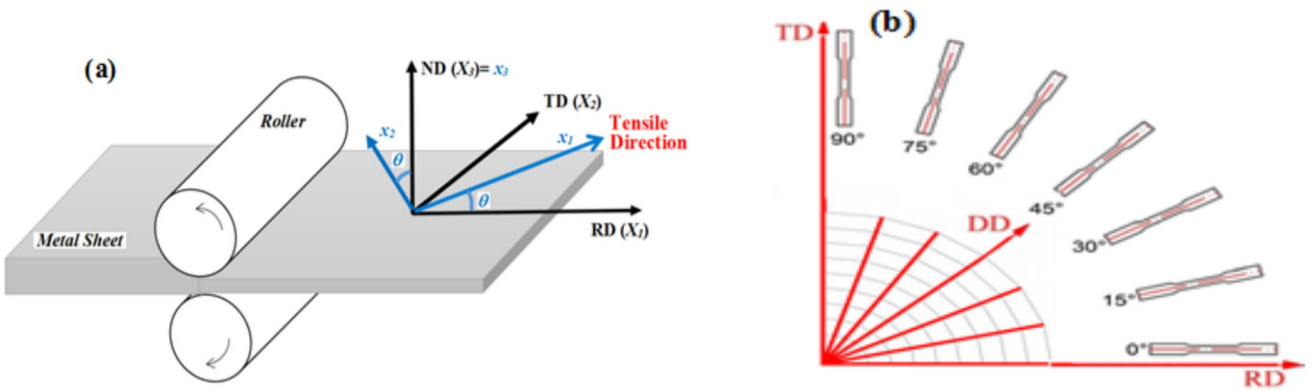


**Fig. 1** (a) Overall rolling sheet, (b) Rectangular samples for tensile tests

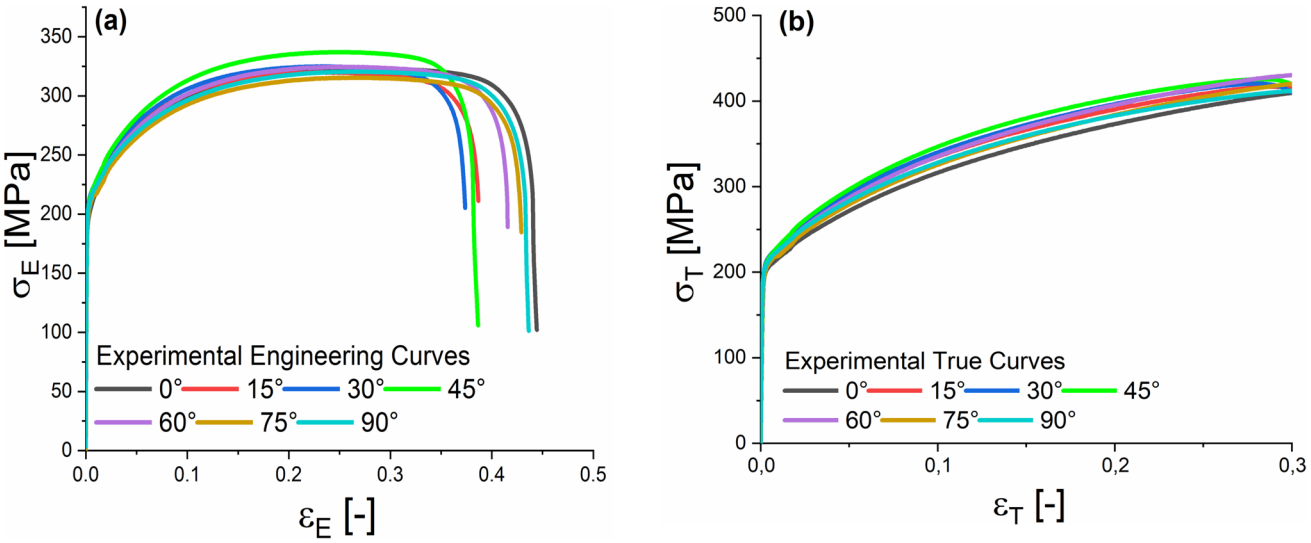


**Fig. 2** Experimental uniaxial Stress–Strain curve of DC04 steel sheet for: (a) Engineering tensile test, (b) True tensile test

direction and the rolling direction (RD) varying from 0° to 90° in 15° increments. Two distinct deformation regimes are observed during the tensile strength measurements. First, the elastic regime is characterised by a proportional limit, where the relationship between stress and strain is linear. In this region, the material tends to return to its original shape after elongation or contraction. Subsequently, at the yield point, the stress transitions into the plastic regime, where the deformation becomes large and permanent until reaching the maximum engineering stress (Ultimate Tensile Strength). This stage is referred to as work hardening. The conversion from engineering to true stress–strain values is given by the Cauchy stress tensor: $\sigma_T = \frac{F}{A} = \sigma_E(\varepsilon_E + 1))$ and the true strain tensor: $\varepsilon_T = \int_{L_0}^{L} \frac{\Delta L}{L} = ln(\varepsilon_E + 1)$.

Where the subscripts $E$ and $T$ denote *Engineering* and *True*, respectively. Here, $F$ is the applied force, and $A$ is the instantaneous cross-sectional area.

Table 2 presents the weighted average of the experimental Lankford coefficient (also called the plastic anisotropy parameter), calculated as: $\bar{r} = (r_0 + 2r_{45} + r_{90})/4 = 1.9125$. This normal anisotropy quantifies the variation between in-plane and through-thickness mechanical properties of the sheet metal. Additionally, the planar anisotropy ($\Delta r$), which influences the earring amplitude in deep-drawn cups, was determined as: $\Delta r = (r_0 - 2r_{45} + r_{90})/4 = 0.445$. Notably, earring defects do not occur when the in-plane anisotropy coefficient $r(\theta)$ remains constant across all tested directions.

Under the initial anisotropy, the experimental normalised parameters (flow stress and *r-value*) according to the rolling direction (RD) are listed in Table 3.

To provide a clearer representation of anisotropy in metal sheets, polar coordinate plots are widely used. Figure 3 illustrates the anisotropic behaviour of DC04 sheet metal in such a polar coordinate system. For isotropic materials, both the normalised yield stress $\sigma(\theta)$ and Lankford coefficient $r(\theta)$ would equal 1 at all angles, resulting in a perfect circle on the polar plot. The contours of $\sigma(\theta)$ and $r(\theta)$ deviate from circularity, reflecting directional dependence as the orientation varies from 0° (RD) to 90° (TD). The DC04 sheet exhibits orthotropic symmetry, evidenced by two mutually

**Table 2** Mechanical proprieties of the DC04 steel

| $\nu$ | $\theta(^\circ)$ | $\sigma_{e0.2}(MPa)$ | $\sigma_b(MPa)^a$ | $r(\theta)$ | $(r_b)^b$ | $\bar{r}$ | $\Delta r$ | $H_V$ |
|---|---|---|---|---|---|---|---|---|
| 0.3 | 0° | 206.36 | 204.74 | 1.91 | 0.778 | 1.91 | 0.445 | 134 |
| | 15° | 208.36 | | 1.80 | | | | 135 |
| | 30° | 211.86 | | 1.74 | | | | 139 |
| | 45° | 214.83 | | 1.69 | | | | 165 |
| | 60° | 205 | | 1.86 | | | | 139 |
| | 75° | 203 | | 2.11 | | | | 135 |
| | 90° | 203.13 | | 2.36 | | | | 130 |

[a]_ the equibiaxial flow stress (EB) determined from:$\sigma_b = (\sigma_0 + \sigma_{90})/2$

[b]– the $r_b$-*value* was calculated from Yld96 [13]

**Table 3** The normalised values of the Yield stresses and *r-values* calibrated with respect to the reference direction (RD)

| | | | | | | | | |
|---|---|---|---|---|---|---|---|---|
| Yield stress $\sigma(\theta)$ | $\frac{\sigma_0}{\sigma_0}$ | $\frac{\sigma_{15}}{\sigma_0}$ | $\frac{\sigma_{30}}{\sigma_0}$ | $\frac{\sigma_{45}}{\sigma_0}$ | $\frac{\sigma_{60}}{\sigma_0}$ | $\frac{\sigma_{75}}{\sigma_0}$ | $\frac{\sigma_{90}}{\sigma_0}$ | $\sigma_b$ |
| | 1 | 1 | 1.02 | 1.041 | 0.99 | 0.983 | 0.98 | 0.9921 |
| $r$-value $r(\theta)$ | $\frac{r_0}{r_0}$ | $\frac{r_{15}}{r_0}$ | $\frac{r_{30}}{r_0}$ | $\frac{r_{45}}{r_0}$ | $\frac{r_{60}}{r_0}$ | $\frac{r_{75}}{r_0}$ | $\frac{r_{90}}{r_0}$ | $r_b$ |
| | 1 | 0.942 | 0.910 | 0.884 | 0.973 | 1.010 | 1.235 | 0.778 |

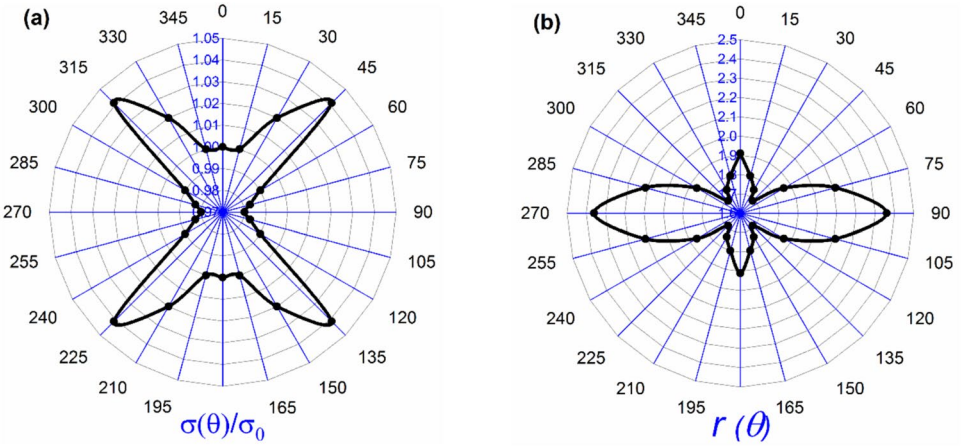


**Fig. 3** Anisotropy parameters change under different Loading directions for: (a) normalised yield stress, (b) Lankford value

perpendicular planes of symmetry aligned with the rolling (RD = 0°) and transverse (TD = 90°) directions. This is confirmed by the mirror symmetry of the polar diagram about these axes.

## Hardness mechanical testing

An early work by Tabor [39, 40] established an empirical relationship between Vickers hardness (*Hv*) and flow strength, $\sigma_0$, approximated by the expression given in Eq. (1).

$$H_v \approx 3\sigma_0 \tag{1}$$

Recently, Zhang & Zhang [43] analysed the relationship between hardness and ultimate tensile strength (UTS), demonstrating that for many materials, the Vickers hardness (*Hv*) approximates three times the UTS, with the *Hv*/UTS ratio typically ranging from 2.3 to 3.7.

The Vickers hardness of the DC04 sheet material was measured using a digital micro-hardness tester (INNOVATEST). Prior to testing, all sample surfaces were mechanically polished to a mirror finish using 2000-grit metallographic abrasive paper. Hardness measurements were performed by: i) Applying a 10 kgf (98.07 N) load for 20 s, ii) Measuring the resulting indentations ($d_1$ and $d_2$) using optical microscopy, and iii) Repeating the process six times per specimen. The Vickers hardness number was calculated using the standard formula:

$$H_v = 1.854\frac{F}{d^2}\ [Kgf/mm^2] \tag{2}$$

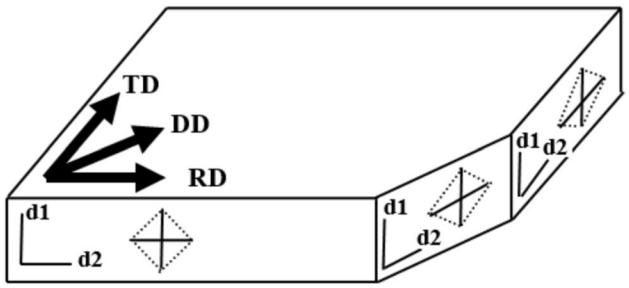


**Fig. 4** Faces of Vickers hardness tests

where $d$ is mean diagonal length $(d1 + d2)/2$, in $(mm)$ and $F$ is the applied force in kilograms-force $(Kgf)$. Initially, all seven specimens were oriented along their thickness direction in the (ND-θ°) planes (Fig. 4) before hardness characterisation. Vickers hardness measurements were subsequently performed on each prepared surface. The Vickers indentation was systematically oriented such that:

(i) The primary diagonal ($d1$) remained consistently aligned with the normal direction (ND).
(ii) The secondary diagonal ($d2$) was incrementally rotated from 0° to 90° in 15° intervals relative to the rolling direction (RD).

## Yield criteria description

Uniaxial tensile testing offers valuable insights into plastic flow limits, with stress–strain curves providing a clear interpretation of material behaviour under single-direction loading.

However, characterizing multiaxial stresses introduces notable challenges, including greater mechanical complexity, non-uniform strain distributions, and extensive experimental time requirements. In these scenarios, plastic flow functions serve as a practical alternative, allowing for accurate prediction of anisotropic mechanical properties (stress/strain evolution) while significantly reducing experimental effort.

## BBC-2003 yield criterion

In 2003, Banabic et al.[16] proposed the BBC2003 yield criterion to model anisotropic yielding behaviour of sheet metals under plane stress conditions. The criterion's effective yield stress is given by Eq. (3):

$$\sigma_0 = \left[a(\tau+\psi)^{2\chi} + a(\tau-\psi)^{2\chi} + (1-a)(2\Delta)^{2\chi}\right]^{\frac{1}{2\chi}} \tag{3}$$

where:

$$\begin{cases} \tau = \frac{\sigma_{11}+M\sigma_{22}}{2} \\ \psi = \sqrt{\left(\frac{N\sigma_{11}-P\sigma_{22}}{2}\right)^2 + Q^2\sigma_{12}^2} \\ \Delta = \sqrt{\left(\frac{R\sigma_{11}-S\sigma_{22}}{2}\right)^2 + T^2\sigma_{12}^2} \end{cases}$$

## BBC-2005 yield criterion

In 2005, Banabic et al. [17] proposed an enhanced version of the BBC2003 yield criterion, incorporating additional material coefficients to improve the predictive capability. For a general coordinate system, the equivalent stress formulation is given by Eq. (4):

$$\sigma_0 = \left[a(\Delta+\Gamma)^{2\chi} + a(\Delta-\Gamma)^{2\chi} + b(\Delta+\psi)^{2\chi} + b(\Delta-\psi)^{2\chi}\right]^{\frac{1}{2\chi}} \tag{4}$$

With the material parameters $a$, $b>0$, but the $\Gamma$, $\Delta$ and $\Psi$ functions in relation to the planar stress tensor components in the following relation:

$$\begin{cases} \Gamma = L\sigma_{11} + M\sigma_{22} \\ \Delta = \sqrt{\left(N\sigma_{11} - P\sigma_{22}\right)^2 + \sigma_{12}^2} \\ \psi = \sqrt{\left(Q\sigma_{11} - R\sigma_{22}\right)^2 + \sigma_{12}^2} \end{cases}$$

The BBC2005 yield function incorporates 09 key material parameters (a, L, M, N, P, Q, R, S, T, $\chi$) to characterize anisotropic flow behaviour, with the following constraints:

1. Constitutive Parameter Requirements:
2. All parameters (L, M, N, P, Q, R, S, T) must maintain positive values
3. The weighting coefficient $a$ is bounded: $0 \le a \le 1$
4. The non-quadratic exponent $\chi$ takes integer values based on crystal structure:
5. $\chi = 3$ for BCC (body-centered cubic) materials
6. $\chi = 4$ for FCC (face-centered cubic) materials
7. Parameter Determination:
8. Numerical optimization studies by the original authors [18] confirm these parameters yield optimal identification of the yield surface
9. Parameter selection must align with the material's crystallographic texture

## BBC-2008 yield criterion

To enhance the predictive performance and representational capabilities of the BBC2005 yield function [18], Banabic et al. (2008) developed an improved version of this model with greater flexibility. The plane-stress equivalent stress formulation of the BBC2008 yield criterion is expressed in Eq. (5) as follows:

$$\frac{\sigma_0^{2\chi}}{w-1} = \sum_{i=1}^{s}\left[w^{i-1}\left\{(L^i+M^i)^{2\chi} + (L^i-M^i)^{2\chi}\right\} + w^{s-i}\left\{(M^i+N^i)^{2\chi} + (M^i-N^i)^{2\chi}\right\}\right] \tag{5}$$

$\chi, s \in N^*$ $w = (3/2)^{1/s} > 1$

$$\begin{cases} L^i = l_1^i\sigma_{11} + l_2^i\sigma_{22} \\ M^i = \sqrt{\left(m_1^i\sigma_{11} - m_2^i\sigma_{22}\right)^2 + m_3^i\left(2\sigma_{12}\right)^2} \\ N^i = \sqrt{\left(n_1^i\sigma_{11} - n_2^i\sigma_{22}\right)^2 + n_3^i\left(2\sigma_{12}\right)^2} \end{cases}$$

These coefficients: $l_1^i, l_2^i, m_1^i, m_2^i, m_3^i, n_1^i, n_2^i, n_3^i$ represent anisotropic plasticity parameters requiring experimental identification.

### Constitutive relations for oriented loading

When the sample axis is rotated by an angle $\theta$ relative to the rolling direction (RD), the resulting uniaxial tensile stress $\sigma(\theta)$ along the $\theta$-direction can be expressed as:

$$\begin{cases} \sigma_{11} = \sigma(\theta)\cos^2\theta \\ \sigma_{22} = \sigma(\theta)\cos^2\theta \\ \sigma_{12} = \sigma(\theta)sin\theta cos\theta \end{cases} \tag{6a}$$

where $\sigma_{11}$, $\sigma_{22}$, and $\sigma_{12}$ are plane components of Cauchy stress tensor that can be determined from coordinate rotations. Under balanced biaxial tensile test, the $\sigma_b$ yield stress components are:

$$\begin{cases} \sigma_{11} = \sigma_b \\ \sigma_{22} = \sigma_b \\ \sigma_{12} = 0 \end{cases} \tag{6b}$$

### Theoretical anisotropy coefficient prediction

The plastic strain ratio $r(\theta)$, which characterizes material anisotropy at orientation (θ) relative to the rolling direction, is determined by [37]:

$$r(\theta) = \frac{\dot{\varepsilon}_{yy}}{\dot{\varepsilon}_{zz}} = -\frac{(\frac{f(\sigma_{ij})}{\partial\sigma_{xx}}).\sin^2\theta - (\frac{f(\sigma_{ij})}{\partial\sigma_{xy}}).\sin 2\theta + (\frac{f(\sigma_{ij})}{\partial\sigma_{yy}}).\cos^2\theta}{\frac{f(\sigma_{ij})}{\partial\sigma_{xx}} + \frac{f(\sigma_{ij})}{\partial\sigma_{yy}}} \tag{7a}$$

The equibiaxial $r_b$ is defined as

$$r_b = \frac{f(\sigma_{ij})}{\partial\sigma_{yy}} \Big/ \frac{f(\sigma_{ij})}{\partial\sigma_{xx}} \tag{7b}$$

### Anisotropy coefficient of Yld96 yield function

For equibiaxial tension ($\sigma_{11} = \sigma_{22}$), the plastic anisotropy ratio $r(\theta)$ is derived from Eq. (8) as the slope $m(\theta) = r_b = \varepsilon_{yy}/\varepsilon_{xx}$. In this study, we adopt the formulation originally developed by Barlat et al. (Yld96) [13], which provides the following specific expressions for calculation:

$$\begin{aligned} r_b = [&-\alpha_x(c_3 + 2c_1)(2c_1 + c_2)\left|2c_1 + c_2\right|^{a-2} + \alpha_y(c_3 - c_1)(c_1 + 2c_2)\left|c_1 + 2c_2\right|^{a-2} - (2c_3 + c_1)(c_1 - c_2) \\ &\left|c_1 - c_2\right|^{a-2}]/[-\alpha_x(c_2 - c_3)(2c_1 + c_2)\left|2c_1 + c_2\right|^{a-2} - \alpha_y(2c_2 + c_3)(c_1 + 2c_2)\left|c_1 + 2c_2\right|^{a-2} \\ &+(c_2 + 2c_3)(c_1 - c_2)\left|c_1 - c_2\right|^{a-2}] \end{aligned} \tag{8}$$

where the non-quadratic integer $a$ is a material-dependent constant with ($a = 8$ for face-centered cubic (FCC) structures and $a = 6$ for body-centered cubic (BCC) structures). On the other side, the coefficients $c_1$, $c_2$, $c_3$, $c_6$, $\alpha_x$, $\alpha_y$ and $\alpha_z$ are determined through numerical optimization using the Newton–Raphson method. The calibrated anisotropy coefficients for DC04 steel are presented in Table 4.

### Material parameter optimization

The anisotropic parameters for the BBC2003, BBC2005, BBC2008_8p, and BBC2008_16p yield functions were determined through nonlinear optimization using the Levenberg–Marquardt least squares algorithm [44, 45]. This numerical implementation was performed in MATLAB™, with the parameter identification based on Eq. (9):

$$\begin{aligned} Error = &\sum_{i=1}^{k}\left[\frac{\sigma_i^{theo}(\theta)}{\sigma_i^{\exp}(\theta)} - 1\right]^2 + \sum_{i=1}^{k}\left[r_i^{theo}(\theta) - r_i^{\exp}(\theta)\right]^2 \\ &+ \sum_{i=1}^{k}\left[\frac{\sigma_i^{theo}(b)}{\sigma_i^{\exp}(b)} - 1\right]^2 + \sum_{i=1}^{k}\left[r_i^{theo}(b) - r_i^{\exp}(b)\right]^2 \end{aligned} \tag{9}$$

The total number of experimental data points used in the parameter identification is denoted by ''*k*''. The superscript *'theo'* indicates values predicted by the BBC yield functions (2003, 2005, 2008_8p, and 2008_16p versions), while *'exp'* marks the corresponding experimentally measured values.

### Validation of the BBC yield criterions

For the as-received material, the numerical characterisation of anisotropic material parameters of BBC yield criterions family is summarized in Table 5 as:

Following calibration across multiple material orientations relative to the rolling direction (RD), Fig. 5 presents the distributions of normalised tensile properties as well as flow stresses and potential loci of BBC family yield criteria under associated and non-associated flow rules compared to the experimental measurements. The prediction of the variation in flow stress along different load directions in the plane of the sheet is shown in Fig. 5 (a, c); with a poor prediction reported on the BBC2005 criterion under the AFR hypothesis and the BBC2008-8p criterion under the non-AFR assumption (s-based model). The anisotropy in the uniaxial tension yield

**Table 4** Yld96 coefficients for DC04 (exponent a = 6)

| $c_1$ | $c_2$ | $c_3$ | $c_6$ | $\alpha_x$ | $\alpha_y$ | $\alpha_z$ |
|---|---|---|---|---|---|---|
| 1.0283 | 0.9874 | 1.0125 | 0.8913 | 0.3969 | 0.5677 | 1.3087 |

**Table 5** Coefficients of the yield criteria for identification strategies

| AFR (Associated Flow rule) | | | | | | | | | |
|---|---|---|---|---|---|---|---|---|---|
| BBC2003 | $\chi=3$ | $a$ | $M$ | $N$ | $P$ | $Q$ | $R$ | $S$ | $T$ |
| | | 0.4811 | 1.0232 | 0.8641 | 0.7959 | 0.8449 | 1.0473 | 1.0628 | 1.0388 |
| BBC2005 | | $a$ | $b$ | $L$ | $M$ | $N$ | $P$ | $Q$ | $R$ |
| | | 0.4737 | 0.7990 | 0.4927 | 0.5056 | 0.4319 | 0.3984 | 0.5472 | 0.5621 |
| BBC2008-8P | | $l_1^1$ | $l_2^1$ | $m_1^1$ | $m_2^1$ | $m_3^1$ | $n_1^1$ | $n_2^1$ | $n_3^1$ |
| | | 0.4994 | 0.5060 | 0.4356 | 0.4035 | 0.3919 | 0.6133 | 0.6880 | 0.6160 |
| BBC2008-16P | | $l_1^1$ | $l_2^1$ | $m_1^1$ | $m_2^1$ | $m_3^1$ | $n_1^1$ | $n_2^1$ | $n_3^1$ |
| | | 0.1896 | 0.2446 | 0.8352 | 0.2815 | 0.3408 | 0.2385 | 0.8741 | 0.4604 |
| | | $l_1^2$ | $l_2^2$ | $m_1^2$ | $m_2^2$ | $m_3^2$ | $n_1^2$ | $n_2^2$ | $n_3^2$ |
| | | 0.3276 | 0.2370 | 0.5798 | 0.7620 | 0.3940 | 0.3697 | −0.0598 | 0.7183 |
| non-AFR_*S* (non-AFR, Stress based model) | | | | | | | | | |
| BBC2003 | $\chi=3$ | $a$ | $M$ | $N$ | $P$ | $Q$ | $R$ | $S$ | $T$ |
| | | 0.3849 | 1.0289 | 0.9567 | 0.6970 | 0.4464 | 1.0170 | 1.0691 | 1.0466 |
| BBC2005 | | $a$ | $b$ | $L$ | $M$ | $N$ | $P$ | $Q$ | $R$ |
| | | 0.2558 | 0.3790 | 0.1975 | 0.9289 | 0.2972 | 0.2860 | 0.8735 | 0.5743 |
| BBC2008-8P | | $l_1^1$ | $l_2^1$ | $m_1^1$ | $m_2^1$ | $m_3^1$ | $n_1^1$ | $n_2^1$ | $n_3^1$ |
| | | 0.2707 | 0.8658 | 0.3505 | 0.4106 | 0.5968 | 0.8833 | 0.2528 | 0.2090 |
| non-AFR _r (non-AFR, Potential plastic-based model) | | | | | | | | | |
| BBC2003 | $\chi=3$ | $a$ | $M$ | $N$ | $P$ | $Q$ | $R$ | $S$ | $T$ |
| | | 0.4313 | 0.9701 | 1.0361 | 1.0036 | 1.0855 | 1.1339 | 1.0301 | 1.0658 |
| BBC2005 | | $a$ | $b$ | $L$ | $M$ | $N$ | $P$ | $Q$ | $R$ |
| | | 0.7606 | 0.4013 | 0.3587 | 0.3627 | 0.2831 | 0.2577 | 0.5068 | 0.6127 |
| BBC2008-8P | | $l_1^1$ | $l_2^1$ | $m_1^1$ | $m_2^1$ | $m_3^1$ | $n_1^1$ | $n_2^1$ | $n_3^1$ |
| | | 0.5274 | 0.6407 | 0.3111 | 0.1506 | 0.3248 | 0.6718 | 0.9582 | 0.7708 |

stress can be reasonably described by all of the yield criteria, which has been successfully validated. The normalised *r-values* determined by these yield criteria were compared to the results of the experiments in Fig. 5 (b, d). To predict the *r-value* directionality, we observed a small difference between the test data and the calculation results of the BBC2003 model under AFR conditions.

To visualise the yield behaviour while neglecting in-plane shear stress, Fig. 6 compares the initial yield loci on the principal stress plane for both theoretical three-flow criteria and experimental results. Under the associated flow rule (AFR), the BBC yield criteria show nearly superimposed flow surfaces, confirming their consistent anisotropic prediction. In contrast, the non-Associated Flow Rule (non-AFR) decouples the yield function from the plastic potential, with significant divergence observed between its s-based (stress-driven) and *r*-based (anisotropy-driven) implementations. Notably, the non-AFR models exhibit reduced accuracy in predicting initial plastic behaviour compared to AFR, particularly for early yielding transitions. This comparison highlights the critical role of flow rule selection in modeling anisotropic plasticity.

## Flow curves of DC04

The mechanical behaviour of DC04 sheet was characterized through tensile stress–strain curves obtained along seven orientations relative to the rolling direction, with strain-hardening parameters optimized for isotropy. The flow stress evolution was best represented by the Hockett-Sherby model [46] (Eq. 10), which provided the best fit to the experimental uniaxial hardening data. This formulation reliably captures the true stress–strain response across all tested directions, reflecting its adaptability in modeling the material's isotropic hardening behaviour while accommodating directional differences in plastic deformation.

$$\begin{cases} \sigma_t(\theta) = \sigma_{sat}(\theta) - \left(\sigma_{sat}(\theta) - \sigma_0(\theta)\right)\exp\left(-c(\theta)\epsilon_t^{h(\theta)}\right) \\ \sigma_b = \sigma_{sat}(b) - (\sigma_{sat}(b) - \sigma_0(b))exp(-c_b\epsilon_t^{h_b}) \end{cases} \quad (10)$$

The Hockett-Sherby hardening model requires calibration of four orientation-dependent parameters (reference yield stress$\sigma_0(\theta)$, saturation stress$\sigma_{sat}(\theta)$, and hardening coefficients$c(\theta)/h(\theta)$) for seven sheet orientations (θ = 0°–90° in 15° increments), and four equivalent biaxial

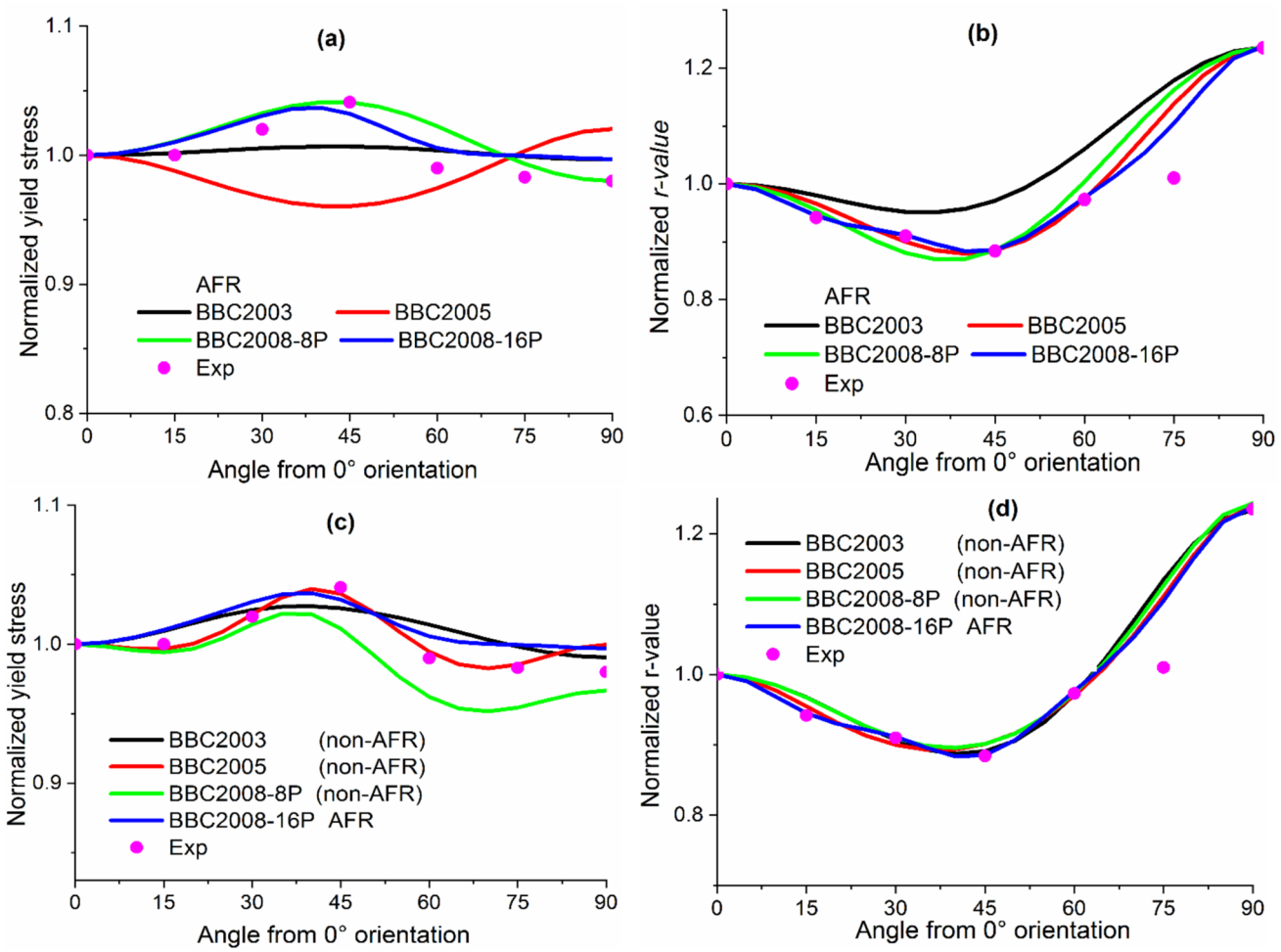


**Fig. 5** Normalised Tensile properties DC04 predicted by the BBC family yield criteria at various directions: (a) Yield stress under *AFR,* (b) *r-value* under *AFR*, (c) Yield stress under non-*AFR* except BBC _16p, and (d) *r-value* under non-*AFR* except BBC _16p

parameters $(\sigma_{sat}(b), \sigma_0(b), c_b, h_b)$. Parameter identification was achieved via least-squares optimization against experimental data, using the rolling direction (RD) uniaxial curve (Fig. 7a) as the reference hardening path. Figure 7-b presents the successfully fitted parameters for all orientations and the equibiaxial flow curve $(\sigma_b)$, demonstrating the model's consistent accuracy in capturing both uniaxial and biaxial plastic deformation across all tested directions.

The fitting data for Hockett-Sherby hardening law relative to seven orientations distributed in the plane and equibiaxial flow curve $\sigma_b$ of the sheet are listed in Table 6 as below:

Using the following equation, derive the corresponding total uniaxial tensile longitudinal $\varepsilon^t_{xx}(\theta)$ and transverse $\varepsilon^t_{yy}(\theta)$ strains:

$$\begin{cases} \varepsilon^t_{xx} = \ln\left(\frac{L_f}{L_0}\right) \\ \varepsilon^t_{yy} = ln(b_f/b_0) \end{cases}$$

where $L$ and $b$ are the measured displacements gauge length and width of the samples, respectively. Therefore, the plastic strains can be calculated using the three orthotropic axes ($x$, $y$, and $z$) as follows:

$$\begin{cases} \varepsilon_{xx}(\theta) = \varepsilon^t_{xx} - \sigma_{xx}/E \\ \varepsilon_{yy}(\theta) = \varepsilon^t_{xx} + \nu\sigma_{xx}/E \end{cases}$$

The elastic properties were defined by a Young's modulus of $E = 200$ GPa and a Poisson's ratio of $\nu = 0.3$. The Lankford coefficients, commonly termed $r(\theta)$-values, serve as the primary parameters for characterizing anisotropic behaviour. These coefficients are determined from uniaxial tensile tests by measuring the true strain ratio between the thickness and transverse directions. Due to the strong resistance of materials to volume changes (plastic incompressibility), this principle is often applied in calculating $r(\theta)$-values, as expressed by the following relationship:

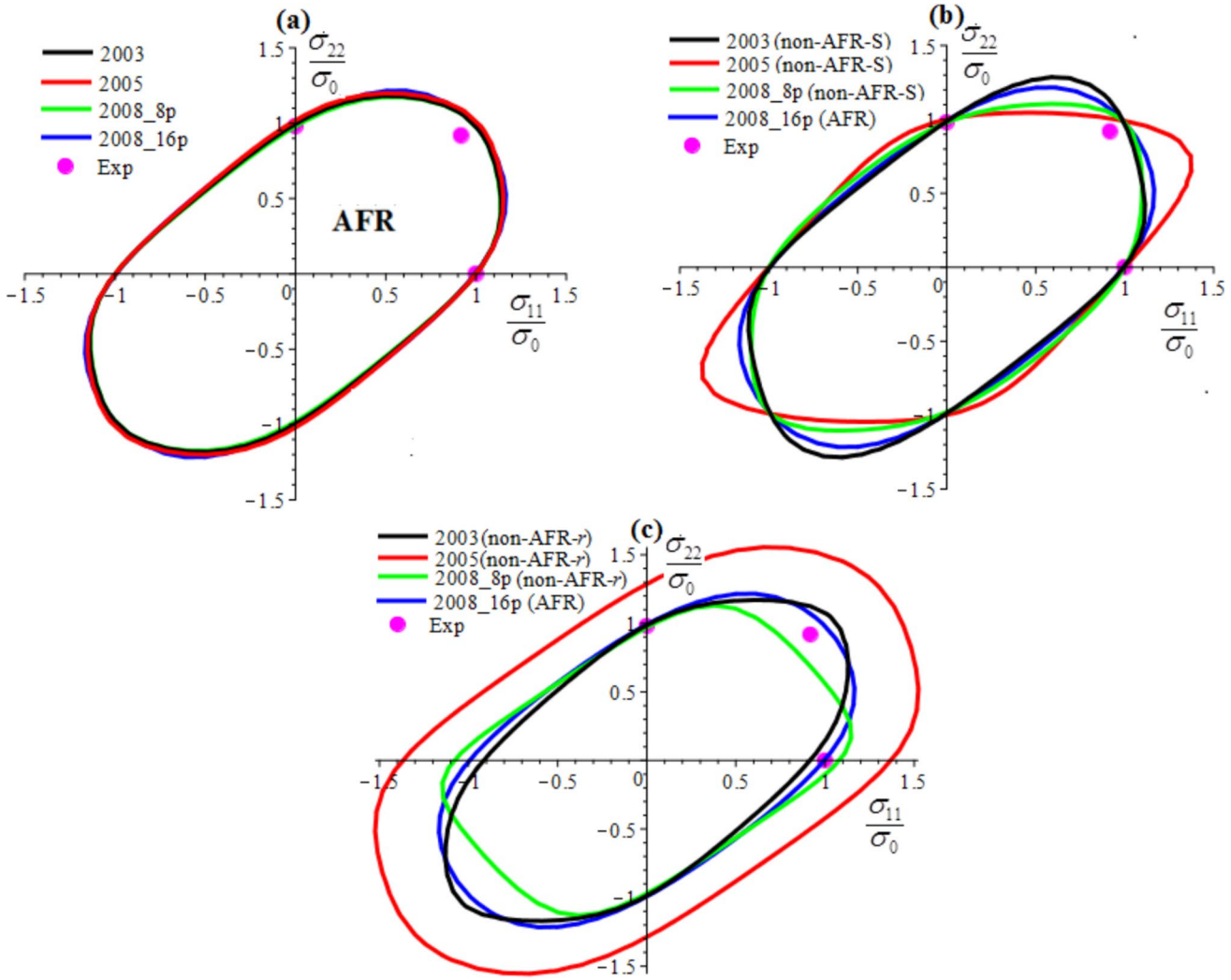


**Fig. 6** Comparison of the predicted yield and potential surfaces under the neglect of the shear stress (contours for $\sigma_{12} = 0$) in the plane of the sheet under: (a) AFR approach, (b) non-AFR_*S* approach, and (c) non-AFR_*r* approache except BBC 2008_16p criterion

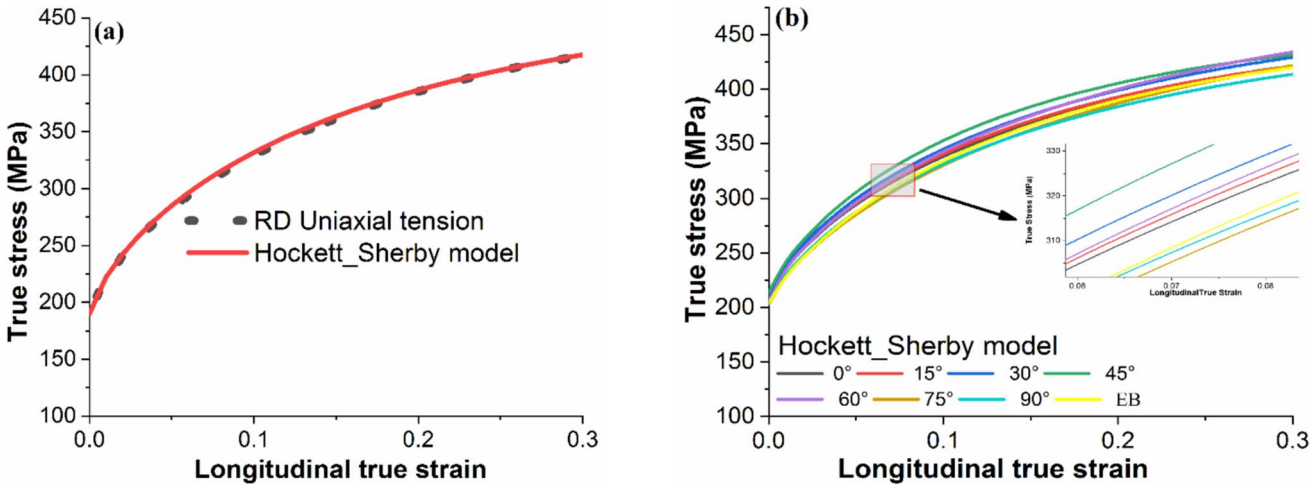


**Fig. 7** Experimental hardening curve fitting using the Hockett-Sherby model: (a) According to the RD uniaxial tension and (b) Prediction at various orientations and biaxial extension

**Table 6** Fitted constants for the Hockett-Sherby hardening formulate by Eq. (10)

| Orientation | Hockett-Sherby model | | | |
|---|---|---|---|---|
| | $\sigma_{sat}(MPa)$ | $\sigma_0(MPa)$ | $c$ | $h$ |
| 0° | 478 | 206 | 3.9 | 0.767 |
| 15° | 468 | 208 | 4.5 | 0.8 |
| 30° | 484 | 211 | 4.15 | 0.788 |
| 45° | 466 | 214 | 5.42 | 0.83 |
| 60° | 512 | 205 | 3.43 | 0.76 |
| 75° | 500 | 203 | 3.45 | 0.79 |
| 90° | 469 | 203 | 4.07 | 0.79 |
| $\sigma_b$ | 464 | 204 | 4.95 | 0.852 |

***r*(θ)-values**

$$r(\theta)_{instantanous} = \frac{\varepsilon_w(\theta)}{\varepsilon_t(\theta)} = \frac{\varepsilon_{yy}(\theta)}{\varepsilon_{zz}(\theta)} = \frac{\varepsilon_{yy}(\theta)}{-(\varepsilon_{xx}(\theta)+\varepsilon_{yy}(\theta))} = \frac{-\mathrm{m}(\theta)}{(1+\mathrm{m}(\theta))} \text{ with} \varepsilon_{xx}(\theta)+\varepsilon_{yy}(\theta)+\varepsilon_{zz}(\theta)=0 \quad (11)$$

where $\varepsilon_{xx}$, $\varepsilon_{yy}$ and $\varepsilon_{zz}$ represent the true plastic strains in the rolling, transverse, and thickness directions, respectively, as measured in uniaxial tensile tests. The slope $m(\theta)$, determined via linear regression of the optimized strain curve, quantifies the relationship between transverse and longitudinal true plastic strains. Following Eq. (11) and in accordance with British Standard ISO 10113:2006, the plastic anisotropy coefficient $r(\theta)$ is derived from the ratio of true transverse strain to true plastic longitudinal strain.

The experimental results obtained from this equation correspond to the instantaneous *r*-value, which evolves continuously from the onset of plastic deformation. A linear relationship between the two strain components persists up to approximately 20% strain within the uniform deformation regime, as illustrated in Fig. 8.

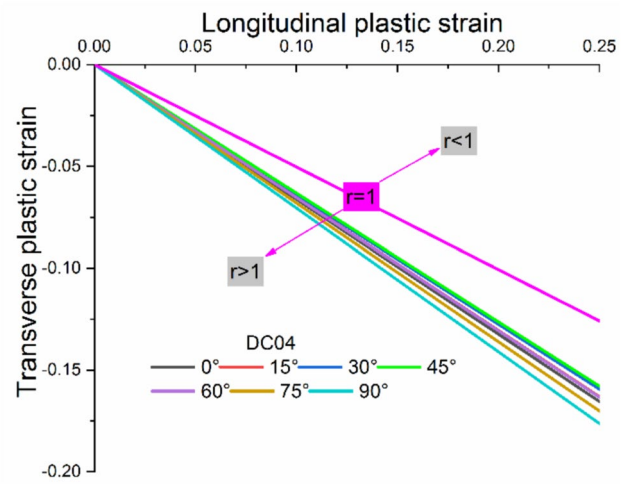


**Fig. 8** True plastic transverse to longitudinal strain ratios at seven angles measured experimentally

For each orientation, the relationship between transverse and longitudinal plastic strains was modelled using a first-degree polynomial (Eq. 12). The evolution of the experimental Lankford parameter follows a linear function expressed as:

$$\varepsilon_{yy}(\theta) = a + m(\theta)\varepsilon_{xx}(\theta) \quad (12)$$

Table 7 presents the experimentally determined parameters for all seven orientations, along with the derived ratios of transverse to longitudinal true plastic strains. These results were calculated using the relationships defined in Eqs. (11) and (12).

In this section, the longitudinal plastic strain, $\varepsilon^p$, was evaluated over a range of 0.002 to 0.2. The evolution of the Lankford coefficient $r(\theta)$ for DC04 steel, predicted by the proposed regression model, was compared with experimental data across multiple loading directions to characterize its dependence on plastic strain during deformation. The analysis reveals a pronounced influence of both plastic strain $\varepsilon^p$ and material orientation on the anisotropy parameters. Specifically, the $r(\theta)$-values—measured at 15° intervals from 0° to 90°—and the equibiaxial coefficient *rb* exhibit significant dependence on the reference longitudinal equivalent strain $\varepsilon^p$. Figure 9 illustrates the variation of these parameters over the deformation range, as derived from three replicate samples.

The anisotropy parameters were approximated using the following equation:

$$\begin{cases} r(\theta) = A_r(\theta) - B_r(\theta)\exp\left(-C_r(\theta)\varepsilon^p\right) + D_r(\theta)/\varepsilon^p \\ r_b = A_r(b) - B_r(b)\exp\left(-C_r(b)\varepsilon^p\right) + D_r(b)/\varepsilon^p \end{cases} \quad (13)$$

For DC04 steel, the fitting coefficients $Ar$, $Br$, $Cr$, and $Dr$ were optimized for orientations θ = 0°,15°,30°,45°,60°,75°,90°, along with the equibiaxial coefficients $A_r(b), B_r(b), C_r(b)$and$(b)$. These values are summarized in Table 8. Comparisons with experimental data confirm that the fitted curves accurately describe the

**Table 7** Constants of linear regression

| Angle | $\alpha$ | $m(\theta)$ |
|---|---|---|
| 0° | −0.0022 | −0.6568 |
| 15° | −0.0031 | −0.6429 |
| 30° | −0.0013 | −0.6350 |
| 45° | −0.0014 | −0.6280 |
| 60° | −0.0015 | −0.6503 |
| 75° | −0.0011 | −0.6784 |
| 90° | −0.0014 | −0.7023 |

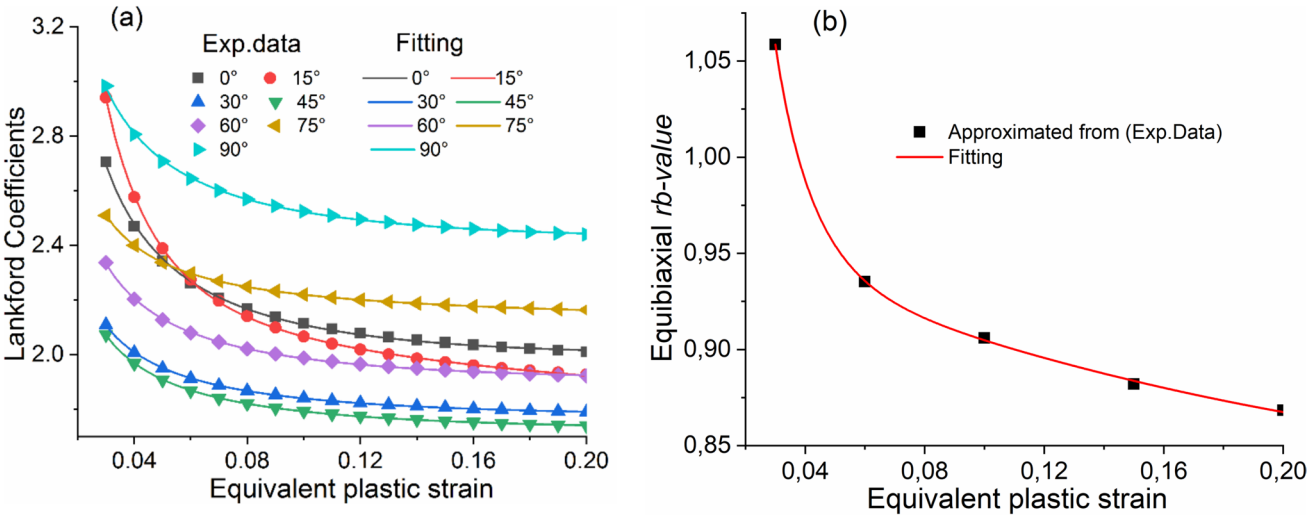


**Fig. 9** (a) Changing of the Lankford value with the plastic strain at seven directions to the RD and (b) equibiaxial *rb-values* (Yld96)

**Table 8** Fitted constants from Eq. (13)

| Orientation | $A_r$ | $B_r$ | $C_r$ | $D_r$ |
|---|---|---|---|---|
| 0° | 1.8967 | 0.1092 | 10.396 | 0.0255 |
| 15° | 1.7675 | 0.2146 | 10.532 | 0.0373 |
| 30° | 1.7353 | 0.0278 | 10.224 | 0.0116 |
| 45° | 1.6833 | 0.0307 | 10.235 | 0.0121 |
| 60° | 1.852 | 0.0435 | 10.276 | 0.0151 |
| 75° | 2.104 | 0.0289 | 10.226 | 0.0125 |
| 90° | 2.349 | 0.0626 | 10.295 | 0.0198 |
| $r_b$ | 0.799 | 0.4555 | 25.264 | 0.0142 |

material's anisotropic behaviour across all loading directions. The regression model achieves an excellent fit, as evidenced by the dotted-line predicted curve ($R = 0.99$) in Fig. 9.

## Evolution of plastic yielding behaviour

During sheet metal rolling processes, the initial reference stress exhibits a nonlinear evolution as a function of equivalent plastic strain, particularly noticeable at large strain levels within the isotropic work hardening regime. To characterise the anisotropic behaviour, five distinct levels of equivalent plastic strain (0.2%, 3%, 10%, 15%, and 20%) were selected within the homogeneous strain-hardening region for parameter identification.

The anisotropy parameters were determined using instantaneous mechanical properties through application of the BBC yield function family. Figure 10 presents a comparative analysis between experimental yield stresses and predicted yield surfaces, along with corresponding plastic potential surfaces, at the selected plastic strain levels. This comparison evaluates the performance of various BBC criteria formulations under both non-associated (non-AFR) and associated (AFR) flow rule approaches, while neglecting shear stress effects ($\sigma_{12} = 0$) along the rolling direction (RD).

## Correlation between hardness values and anisotropy ratio

The anisotropy ratio can be estimated through the dimensional ratio $\rho = d_2/d_1$, where $d_1$ and $d_2$ represent the indentation diagonal measurements, as proposed by Ohashi et al. [47]. In isotropic materials, these diagonal measurements become equal ($\rho = 1$), while any deviation from unity indicates anisotropic behaviour, in direct analogy with the definition of the Lankford coefficient $r(\theta)$.

The experimental measurements, including hardness values, anisotropy aspect ratio ($\rho$), flow stress, and ultimate tensile strength (UTS) of the sheet steel, are summarized in Table 9. The hardness-to-UTS ratio consistently approximates a value of 3, with a maximum observed absolute deviation of 0.73. For the three principal material directions (RD, TD, and DD), the planar average aspect ratio was calculated as $\overline{\rho} = (\rho_0 + 2\rho_{45} + \rho_{90})/4 = 1.372$, demonstrating the material's anisotropic characteristics.

This study demonstrates that the error reduction in mechanical behaviour characterisation follows a linear relationship. A linear regression applied to the experimental data in Fig. 11-a effectively correlates hardness with maximum tensile stress. The material's anisotropic behaviour was evaluated through hardness variations, measured with diagonal length differences across seven specimen orientations. Hardness values were subsequently determined for seven distinct orientations relative to the

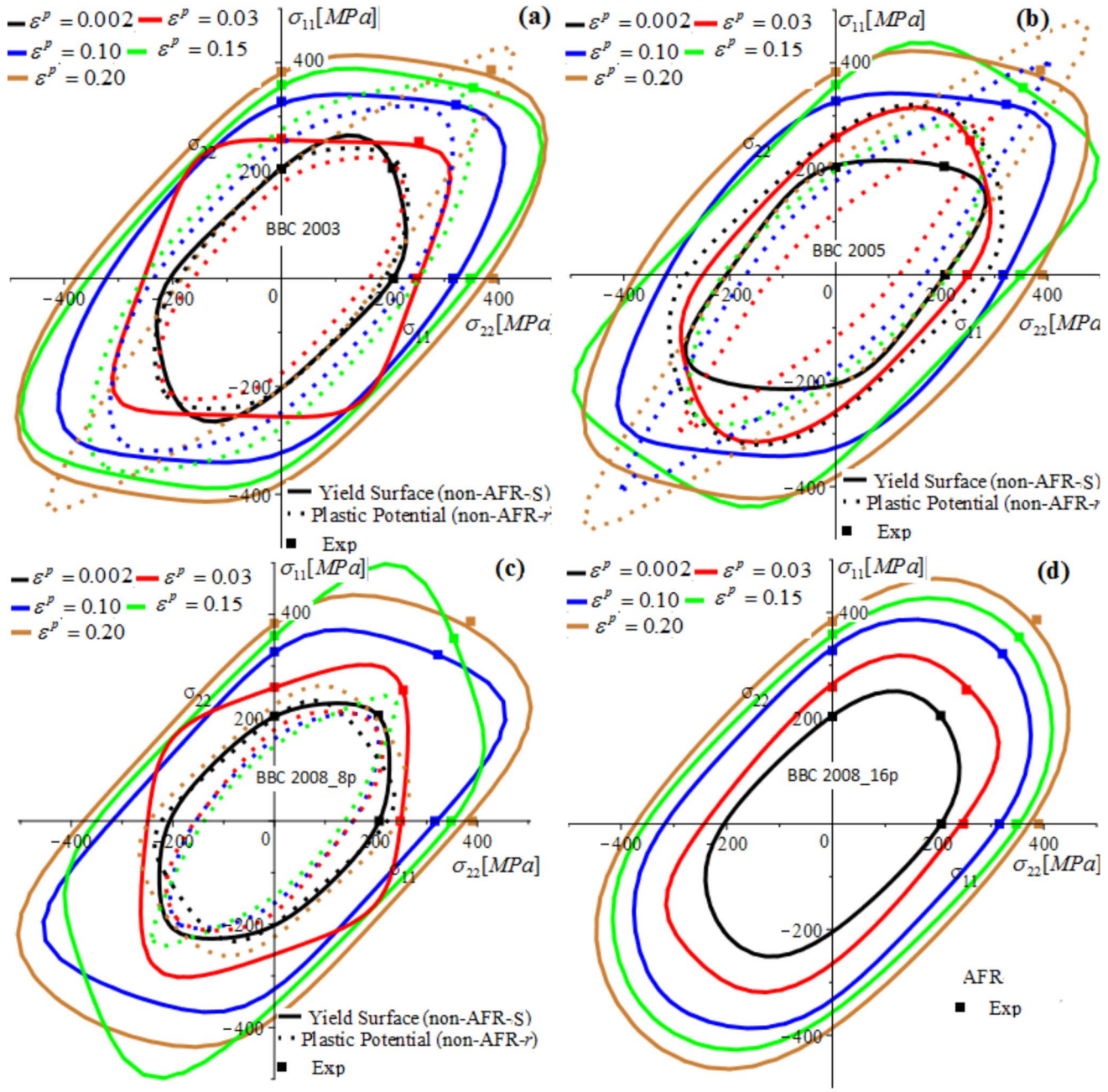


**Fig. 10** Evolution in yield and plastic potential surfaces with increase in effective plastic strain for: (a) BBC 2003, (b) BBC 2005, (c) BBC 2008_8p, and (d) BBC 2008_16p under non-AFR and AFR scheme

(ND-θ°) planes. The angular dependence of hardness relative to the rolling direction (RD) is presented in Fig. 11-b, showing the variation with indentation angle to the normal plane.

A high Lankford coefficient (*r-value*) indicates superior in-plane deformation capability with minimal thickness reduction, making it an effective predictor of deep-drawing performance in sheet metals. The experimental results reveal an average anisotropy parameter ($\bar{r} = 1.91$) significantly exceeding unity. Similarly, the measured surface aspect ratio ($\bar{\rho} = 1.372$) surpasses the isotropic reference value, indicating pronounced anisotropy. This manifests geometrically as the indentation diagonal parallel to the rolling direction ($d_2 \| RD$) being substantially longer than the perpendicular diagonal ($d_1 \perp RD$).

To find a harmonious correspondence between anisotropic and aspect ratio parameters, a modelling calculation is proceeded. Therefore, based on the 2nd order polynomial fit, the regression parameter was proposed for this sheet. the regression model of the 2nd order function is defined by:

**Table 9** The measured hardness values and the anisotropy aspect ratio $\rho$

| $\theta(°)$ | $\sigma_{UTS}$ [MPa] True | $Hv$ [MPa] | $\frac{Hv}{\sigma_{UTS}}$ | $d_1$ [$\mu m$] | $d_2$ [$\mu m$] | $\rho$ [−] | $r(\theta)$ |
|---|---|---|---|---|---|---|---|
| 0 | 413 | 1340 | 3.24 | 35.3 | 37.1 | 1.05 | 1.91 |
| 15 | 416 | 1350 | 3.25 | 35.1 | 39.0 | 1.11 | 1.80 |
| 30 | 425 | 1390 | 3.27 | 33.7 | 39.4 | 1.17 | 1.74 |
| 45 | 425 | 1650 | 3.88 | 28.5 | 38.5 | 1.35 | 1.69 |
| 60 | 430 | 1390 | 3.23 | 30.1 | 42.7 | 1.42 | 1.86 |
| 75 | 422 | 1350 | 3.20 | 29.0 | 46.4 | 1.6 | 2.11 |
| 90 | 412 | 1300 | 3.15 | 27.5 | 48.0 | 1.74 | 2.36 |

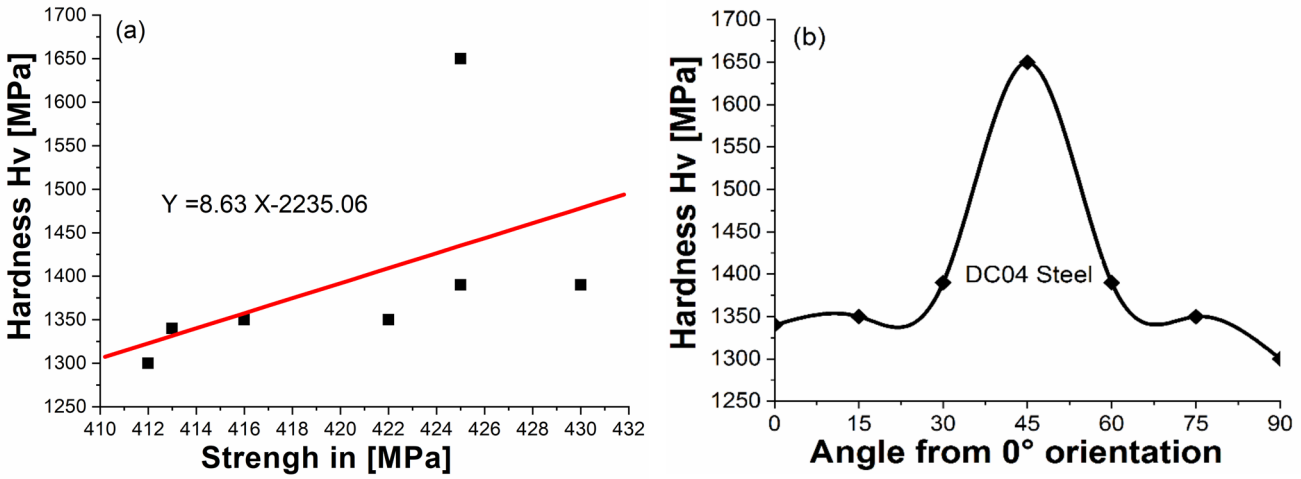


**Fig. 11** (a) Optimum correlation $Hv = f(\sigma_{UTS})$ and (b) Angular dependence of mechanical hardness $Hv$ corresponding to the (ND-$\theta$°) planes

$$r(\theta) = 2.928\rho^2 - 7.421\rho + 6.44 \quad (14)$$

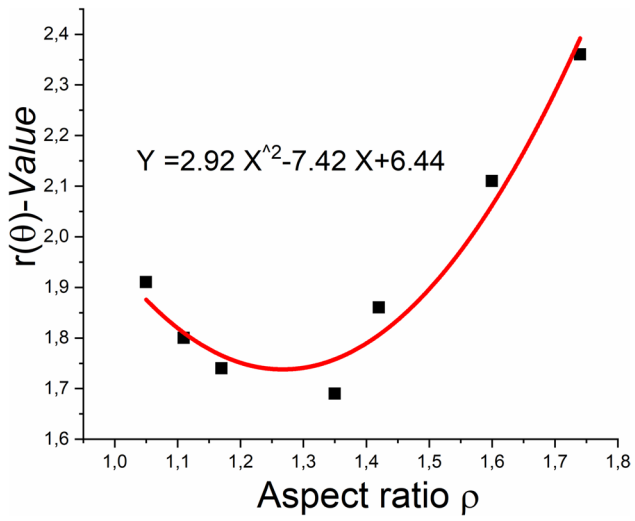


**Fig. 12** Correlation between the Lankford *r-value* and the aspect ratio in the Vickers hardness test

Based on the polynomial relationship linking the anisotropic parameters, the correlation coefficient between $r(\theta)$ and $\rho$ is 0.96169. The polynomial approximation $r(\theta) = f(\rho)$ can be represented by the curve plotted in Fig. 12.

## Conclusions

This study investigated the effect of anisotropic mechanical parameters on the plasticity of cold-strained DC04 ferritic steel sheets. It included experimental work, modelling, analysis, and numerical prediction of the evolution of mechanical properties. A set of three BBC yield functions was proposed to model yield surface evolution under seven different loading orientations. Analytical identification methods were employed to characterise the equibiaxial tension and the balanced Lankford value. Based on the obtained results, the key findings are summarised as follows:

(1) Initial anisotropy: Under both associated and non-associated flow rules, the distribution profiles in the sheet plane of normalised tensile properties, flow stresses,

and potential loci of the BBC yield criteria were examined. The BBC function family harmoniously predicts the material's mechanical behaviour compared to experimental results. Among them, the BBC2008-16p criterion offered the greatest flexibility. With the associated flow rule (AFR), the flow surface contours of the BBC family nearly coincide with the isotropic von Mises case. However, significant discrepancies between the criteria emerge under the non-associated flow rule (non-AFR) assumption.

(2) Evolving anisotropy: The instantaneous evolution of anisotropic behaviour in mechanical properties with respect to selected levels of plastic strain was captured and described. During the rolling process, and within the isotropic work-hardening domain, a method was proposed to estimate the evolution of anisotropic parameters for both stress and strain tensors. The contour surfaces of the BBC family model under both non-AFR and AFR assumptions were predicted for yield and plastic potential surfaces.

(3) Local mechanical properties: Hardness profiles were examined to assess their relationship with material anisotropy. A second-order polynomial fit was applied to establish a correlation between the anisotropic coefficient $r(\theta)$ and the aspect ratio parameter $\rho(\theta)$, ensuring a consistent analytical framework.

## Declarations

**Conflict of interest** The authors declare that they have no conflict of interest.

## References


1. Chahaoui O, Fares ML, Piot D, Montheillet F (2013) Mechanical modeling of macroscopic behaviour for anisotropic and heterogeneous metal alloys. Met Mater Int 19:1005–1019. https://doi.org/10.1007/s12540-013-5013-3
2. Chahaoui O, Matougui N, Boulahrouz S et al (2021) An Associated and Nonassociated Flow Rule Comparison for AISI 439–430TI Forming: Modeling and Experimental Analysis. Lat Am J Solids Struct 18:e406. https://doi.org/10.1590/1679-78256724
3. Chahaoui O, Fares ML, Piot D, Montheillet F (2011) Monoclinic effects and orthotropic estimation for the behaviour of rolled sheet. J Mater Sci 46:1655–1667. https://doi.org/10.1007/s10853-010-4983-5
4. Motaman SAH, Haase C (2021) The microstructural effects on the mechanical response of polycrystals: A comparative experimental-numerical study on conventionally and additively manufactured metallic materials. Int J Plast 140:102941. https://doi.org/10.1016/j.ijplas.2021.102941
5. Regaiguia B, Chahaoui O, Saoudi A et al (2022) An Evolutionary Anisotropic Behavior for DC04 Sheet Using Hill48 Function under Non-Associated Flow Rule Hypothesis. J Nano- Electron Phys 14:05009–1. https://doi.org/10.21272/jnep.14(5).05009
6. Mises RV (1913) Mechanik der festen Körper im plastisch-deformablen Zustand. Nachrichten von der Gesellschaft der Wissenschaften zu Göttingen, Mathematisch-Physikalische Klasse 1913:582–592
7. Hill R (1948) A theory of the yielding and plastic flow of anisotropic metals. Proc R Soc Lond A 193:281–297. https://doi.org/10.1098/rspa.1948.0045
8. Hosford WF (1972) A Generalized Isotropic Yield Criterion. J Appl Mech 39:607–609. https://doi.org/10.1115/1.3422732
9. Hosford WF (1996) On the crystallographic basis of yield criteria. Textures and Microstructures 26–27:479–493
10. Karafillis AP, Boyce MC (1993) A general anisotropic yield criterion using bounds and a transformation weighting tensor. J Mech Phys Solids 41(12):1859–86
11. Barlat F, Lian J (1989) Plastic behavior and stretchability of sheet metals. Part I: A yield function for orthotropic sheets under plane stress conditions. Int J Plast 5:51–66
12. Barlat F, Lege DJ, Brem JC (1991) A six-component yield function for anisotropic materials. Int J Plast 7:693–712. https://doi.org/10.1016/0749-6419(91)90052-Z
13. Barlat F, Maeda Y, Chung K et al (1997) Yield function development for aluminum alloy sheets. J Mech Phys Solids 45:1727–1763. https://doi.org/10.1016/S0022-5096(97)00034-3
14. Barlat F, Becker RC, Hayashida Y et al (1997) Yielding description for solution strengthened aluminum alloys. Int J Plast 13:385–401. https://doi.org/10.1016/S0749-6419(97)80005-8
15. Barlat F, Brem JC, Yoon JW et al (2003) Plane stress yield function for aluminum alloy sheets—part 1: theory. Int J Plast 19:1297–1319. https://doi.org/10.1016/S0749-6419(02)00019-0
16. Banabic D, Kuwabara T, Balan T et al (2003) Non-quadratic yield criterion for orthotropic sheet metals under plane-stress conditions. Int J Mech Sci 45:797–811. https://doi.org/10.1016/S0020-7403(03)00139-5
17. Banabic D, Aretz H, Paraianu L, Jurco P (2005) Application of various FLD modelling approaches. Modelling Simul Mater Sci Eng 13:759–769. https://doi.org/10.1088/0965-0393/13/5/009
18. Comsa D-S, Banabic D (2008) Plane-Stress Yield Criterion for Highly-Anisotropic Sheet Metals
19. Barlat F, Aretz H, Yoon JW et al (2005) Linear transfomation-based anisotropic yield functions. Int J Plast 21:1009–1039. https://doi.org/10.1016/j.ijplas.2004.06.004
20. Hu Q, Yoon JW, Stoughton TB (2021) Analytical determination of anisotropic parameters for Poly6 yield function. Int J Mech Sci 201:106467. https://doi.org/10.1016/j.ijmecsci.2021.106467
21. Aretz H, Barlat F (2013) New convex yield functions for orthotropic metal plasticity. Int J Non-Linear Mech 51:97–111. https://doi.org/10.1016/j.ijnonlinmec.2012.12.007
22. Yoshida F, Hamasaki H, Uemori T (2013) A user-friendly 3D yield function to describe anisotropy of steel sheets. Int J Plast 45:119–139. https://doi.org/10.1016/j.ijplas.2013.01.010
23. Hu Q, Yoon JW, Manopulo N, Hora P (2021) A coupled yield criterion for anisotropic hardening with analytical description under associated flow rule: Modeling and validation. Int J Plast 136:102882. https://doi.org/10.1016/j.ijplas.2020.102882
24. Cazacu O (2018) New yield criteria for isotropic and textured metallic materials. Int J Solids Struct 139–140:200–210. https://doi.org/10.1016/j.ijsolstr.2018.01.036
25. Yoon JW, Lou Y, Yoon J, Glazoff MV (2014) Asymmetric yield function based on the stress invariants for pressure sensitive metals. Int J Plast 56:184–202. https://doi.org/10.1016/j.ijplas.2013.11.008
26. Hu Q, Li X, Han X et al (2017) A normalised stress invariant-based yield criterion: Modeling and validation. Int J Plast 99:248–273. https://doi.org/10.1016/j.ijplas.2017.09.010

27. Lou Y, Zhang S, Yoon JW (2020) Strength modeling of sheet metals from shear to plane strain tension. Int J Plast 134:102813. https://doi.org/10.1016/j.ijplas.2020.102813
28. Yang H, Zhang W, Zhuang X, Zhao Z (2023) Anisotropic plastic flow of low/medium carbon steel plates in different loading conditions: Characterization of the r-value. J Mater Process Technol 321:118159. https://doi.org/10.1016/j.jmatprotec.2023.118159
29. Stoughton TB (2002) A non-associated flow rule for sheet metal forming. Int J Plast 18:687–714. https://doi.org/10.1016/S0749-6419(01)00053-5
30. Stoughton TB, Yoon J-W (2004) A pressure-sensitive yield criterion under a non-associated flow rule for sheet metal forming. Int J Plast 20:705–731. https://doi.org/10.1016/S0749-6419(03)00079-2
31. Stoughton TB, Yoon JW (2006) Review of Drucker's postulate and the issue of plastic stability in metal forming. Int J Plast 22:391–433. https://doi.org/10.1016/j.ijplas.2005.03.002
32. Cvitanić V, Vlak F, Lozina Ž (2008) A finite element formulation based on non-associated plasticity for sheet metal forming. Int J Plast 24:646–687. https://doi.org/10.1016/j.ijplas.2007.07.003
33. Safaei M, Yoon JW, De Waele W (2014) Study on the definition of equivalent plastic strain under non-associated flow rule for finite element formulation. Int J Plast 58:219–238. https://doi.org/10.1016/j.ijplas.2013.09.010
34. Hu Q, Li X, Chen J (2018) On the calculation of plastic strain by simple method under non-associated flow rule. Eur J Mech A Solids 67:45–57. https://doi.org/10.1016/j.euromechsol.2017.08.017
35. Hou Y, Min J, Stoughton TB et al (2020) A non-quadratic pressure-sensitive constitutive model under non-associated flow rule with anisotropic hardening: Modeling and validation. Int J Plast 135:102808. https://doi.org/10.1016/j.ijplas.2020.102808
36. Barlat F, Yoon S-Y (2023) Anisotropic Plasticity During Non-proportional Loading. In: Altenbach H, Ganczarski A (eds) Advanced Theories for Deformation, Damage and Failure in Materials. Springer International Publishing, Cham, pp 63–119
37. Langford WF, Snyder SC, Bausch J (1950) New criteria for predicting the press performance of deep drawing steels. Trans, Amer Soc Metals 42:1197–1232
38. He Z, Zhang K, Zhu H et al (2022) An anisotropic constitutive model for forming of aluminum tubes under both biaxial tension and pure shear stress states. Int J Plast 152:103259. https://doi.org/10.1016/j.ijplas.2022.103259
39. Tabor D (1948) A Simple Theory of Static and Dynamic Hardness. Proc R Soc Lond A 192:247–274
40. Tabor D (1951) The hardness of metals. Oxford University Press, Great Britain
41. Sanders PG, Youngdahl CJ, Weertman JR (1997) The strength of nanocrystalline metals with and without flaws. Mater Sci Eng A 234–236:77–82. https://doi.org/10.1016/S0921-5093(97)00185-8
42. Cheng Y-T, Cheng C-M (2004) Scaling, dimensional analysis, and indentation measurements. Mater Sci Eng R Rep 44:91–149. https://doi.org/10.1016/j.mser.2004.05.001
43. Zhang P, Li SX, Zhang ZF (2011) General relationship between strength and hardness. Mater Sci Eng A 529:62–73. https://doi.org/10.1016/j.msea.2011.08.061
44. Levenberg K (1944) A method for the solution of certain non-linear problems in least squares. Q Appl Math 2:164–168
45. Marquardt DW (1963) An Algorithm for Least-Squares Estimation of Nonlinear Parameters. J Soc Ind Appl Math 11:1963
46. Hockett JE, Sherby OD (1975) Large strain ~efurmatiun of polycrystalline metals at low homologous temperatures. J Mech Phys Solids 23(2):87–98
47. Ohashi K, Utsunomiya H, Matsumoto R (2011) Evaluation of r-value of steels using Vickers hardness test. Journal of Physics